

Four-Electron Reduction of Oxygen Electrocatalyzed by a Mixture of Porphyrin Complexes onto Glassy Carbon Electrode

Leyla Gidi¹, Camila Canales¹, María J. Aguirre², Francisco Armijo¹, and Galo Ramírez^{1, *}

¹ Facultad de Química, Departamento de Química Inorgánica, Pontificia Universidad Católica de Chile, Av. Vicuña Mackenna 4860, Casilla 306, Correo 22, Santiago, Chile.

² Facultad de Química y Biología, Departamento de Química de los Materiales, Universidad de Santiago de Chile USACH. Av. L.B. O'Higgins 3363, Santiago, Chile.

*E-mail: gramirezj@uc.cl

Received: 24 September 2017 / Accepted: 18 November 2017 / Published: 28 December 2017

In this work a new composite electrode for the electrocatalytic reduction of oxygen (ORR) is presented. For this purpose, glassy carbon electrodes (GC) were modified with Co^{II} and Fe^{III} octaethylporphyrins. The system that presents the highest electrocatalytic activity towards ORR is GC modified with a mixture of both octaethylporphyrins in 1:1 volume proportion (GC Co-Fe 1:1) over the GC electrodes modified with Co^{II} and Fe^{III} octaethylporphyrins separately. This modified electrode can reduce O₂ through two reduction processes (four electrons each), by the generation of H₂O as final product, in two active sites of different chemical nature. All the electrodic systems were morphologically characterized by atomic-force microscopy (AFM) and electrically characterized by electrochemical impedance spectroscopy (EIS). It was found that the electroactive system (GC Co-Fe 1:1) presents high differences on its surface and performs the lowest charge transfer resistance (*R*_{ct}) in comparison to the rest of the modified systems and GC itself.

Keywords: Dioxygen reduction, Modified electrode, porphyrin complex mixtures, Electrocatalysis, Synergic effect

1. INTRODUCTION

The electrocatalytic properties of electrodes modified with transition metal macrocyclic complexes for the oxygen reduction reaction (ORR) in aqueous media have been discussed in several studies. In aqueous media, O₂ is reduced mainly through two processes: by 4 electrons with the generation of H₂O and by 2 electrons to produce H₂O₂. In completely aprotic media, transition metal macrocyclic complexes can catalyze the O₂ reduction via 1 electron giving superoxide ions [1]. For the formation of H₂O to happen, the O=O bond, which shows a high dissociation energy (498 kJ/mol) [2-

4], must break. This implies that the generation of water can involve the simultaneous interaction of both oxygen atoms with two active sites in the electrode surface. In this way, the simultaneous interaction of the oxygen atoms with two active sites can decrease the O=O bond energy in the O₂ molecule, favouring its rupture [4]. The electrocatalytic reduction via 4 electrons to give water is intrinsic to biological respiration [5,6] and to fuel cell technology [7,8]. The carbon electrodes, such as glassy carbon (GC), catalyze the ORR via 2 electrons to generate H₂O₂ [1], but when they are modified with some macrocyclic complexes they can be able to generate H₂O directly by a 4-electron transfer [9-13], enabling their use in fuel cells. The macrocyclic complexes such as phthalocyanines have demonstrated to be effective in catalyzing the ORR and show an activity sequence that depends on the central metal as follows [14].

Higher activity Fe (II) > Co (II) > Ni (II) > Cu (II) Lower activity

As can be observed, the Fe and Co phthalocyanines have been reported as the most active ones. The activity of Co phthalocyanines compared to that of Fe is generally lower [15]. However, the opposite trend can be observed for porphyrins, which present a better response for Co than for Fe [16]. It is known that the oxygen coordination to the central metal of porphyrin complexes strongly depends on the availability of *d* orbitals and the electronic density localized in those orbitals [9]. Co and Fe central metals present a higher availability to receive electronic density in *d* orbitals compared to Ni, Cu, or Zn [17]. This might be the reason why the first two metals are better electrocatalysts to perform the ORR.

Porphyrins are MN₄-type macrocycles and, in nature, are capable of carrying out the transportation of O₂ and electron transfer processes in biological systems [14]. Several aspects participate in this behavior. As example, an increase in the electrocatalytic activity of aniline-porphyrin copolymers towards ORR compared to the one of pure homopolymers has been reported [18] showing that the π delocalized surround of the active site is very important in that reaction. On the other hand, it has been determined that the coordination of Ru groups to Co-porphyrin can turn Co porphyrin into an electrocatalyst for the O₂ to H₂O reduction via 4 electrons [19-22] showing the donor effect of Ru to the metal center, Co. These results opens the possibility to achieve a synergic effect in the ORR electrocatalysis by using a mixture of porphyrin complexes of different central metals, giving way to the existence of more than one metallic center on the electrode surface. Consequently, in this study the ORR was carried out by the use of GC electrode modified with mixtures of Co^{II} and Fe^{III} octaethylporphyrins (CoOEP and FeOEP) (Figure 1), aiming to obtain electrocatalysts active towards the reaction in study. The influence of each central metal at using each porphyrin separately and by mixing them was studied. Morphological studies were carried out to check the superficial differences among the different systems generated and electrochemical impedance spectroscopy (EIS) measures were carried out to characterize the electrical properties of the system.

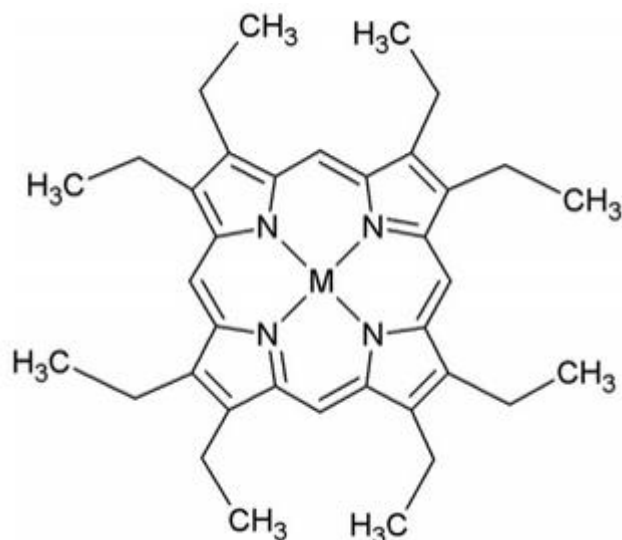


Figure 1. Molecular structure of 2,3,7,8,12,13,17,18-octaethyl-21H,23H-porphyrin, where M = central metal ($\text{Fe}^{\text{III}}\text{OEP}$ and $\text{Co}^{\text{II}}\text{OEP}$).

2. EXPERIMENTAL.

2.1. Reagents and solutions

Sodium hydroxide, hydrogen peroxide, potassium chloride, and dichloromethane were provided by Merck. Argon and dioxygen gases were supplied by AGA, Chile (99.99%). The porphyrins 2,3,7,8,12,13,17,18-octaethyl-21H,23H-porphine cobalt(II) and 2,3,7,8,12,13,17,18-octaethyl-21H,23H-porphine iron(III) chloride were provided by Sigma-Aldrich Chile. Tetra n-butylammonium perchlorate was supplied by TCI America. Deionized water was obtained from a Millipore-Q system (18.2 $\text{M}\Omega\cdot\text{cm}$).

2.2. Equipment

Cyclic voltammetry measurements were carried out by the use of a PalmSens potentiostat. A conventional three-electrode system was used, consisting of a glassy carbon working electrode, a reference electrode Ag/AgCl (3 M KCl), and a platinum counter electrode. The morphological studies were carried out by Innova® Atomic Force Microscope (AFM) using tapping mode. The electrochemical impedance spectroscopy (EIS) technique was applied by using a potentiostat galvanostat CH Instruments 750D.

2.3. Obtaining of modified electrodes

The glassy carbon electrodes (GC) were polished on felt, using alumina slurries (0,3 μm). Later, in order to remove alumina residues and potential contaminants absorbed in the electrode

surface, they were sonicated. To stabilize the electrodes, potential sweeps between -0.6 V and 0.3 V were carried out in a 0.1 M NaOH solution previously saturated with argon obtaining a stable profile. The modification was performed by immersion of the electrode surface, for 30 minutes, in a 0.2 mM CoOEP or FeOEP solution (in CH₂Cl₂), or in a mixture of both octaethylporphyrins (0.2 mM) in different volumetric proportions. Finally, the electrode surfaces were left to dry at room temperature. Once the modified systems were obtained, they were analyzed by potential scanning cycles between -0.9 V and 0.3 V in a 0.1 M NaOH solution previously saturated with O₂ for 20 minutes.

2.4. EIS

In order to carry out the electric characterization of the system by electrochemical impedance spectroscopy, the following parameters were set to perform A.C. A fixed potential at -0.5 V, a frequency range from 100000 Hz to 1 Hz, and amplitude of 0.005 V were used. The measurements were conducted in a 0.1 M NaOH solution previously saturated with O₂ for 20 minutes.

3. RESULTS AND DISCUSSION

3.1. Electroactivity study of different systems

In Figure 2, the voltammetric profiles of each porphyrin in dichloromethane can be observed. According to literature [23,24], the characteristic porphyrin redox processes are observed. CoOEP presents three redox processes assigned to the couples Co^{II}/Co^I (peaks I and II) and Co^{III}/Co^{II} (peak III), in which the peaks I and II would correspond to the redox processes of the central metal, associated to the different geometric arrangements of the porphyrin ligand, specifically to the position of the ethyl groups. This is verified by comparing the sum of the peaks I and II area ($3.833 \cdot 10^{-6} \text{ A} \cdot \text{V}^{-1}$) and the peak III area ($3.901 \cdot 10^{-6} \text{ A} \cdot \text{V}^{-1}$), which is shown in detail in Figure S1 and Table S1 on the supplementary material. These areas can be directly related to the charges of the redox processes and, as they are very similar, they confirm that both the peak I and II would be associated to the Co^{II}/Co^I couple. When all Co is as Co^{II}, the subsequent reduction to Co^I involves all the Co^{II} species. On the other hand, the voltammetric response of FeOEP shows two redox processes corresponding to the Fe^{II}/Fe^I (peak I) and Fe^{III}/Fe^{II} (peak II) couples that are present at more positive potentials compared to CoOEP. In both voltammetric profiles, it is possible to observe signals around -1 V and towards more negative potentials, which are attributed to the response of the porphyrin ligand [23]. Besides, in the case of FeOEP, it is possible to observe cathodic signals between -0.5 and 0.5 V, which have not been assigned yet. On the other hand, it has been determined that the active couple in the oxygen reduction for CoOEP is Co^{III}/Co^{II} and for FeOEP is Fe^{III}/Fe^{II} [12,25,26].

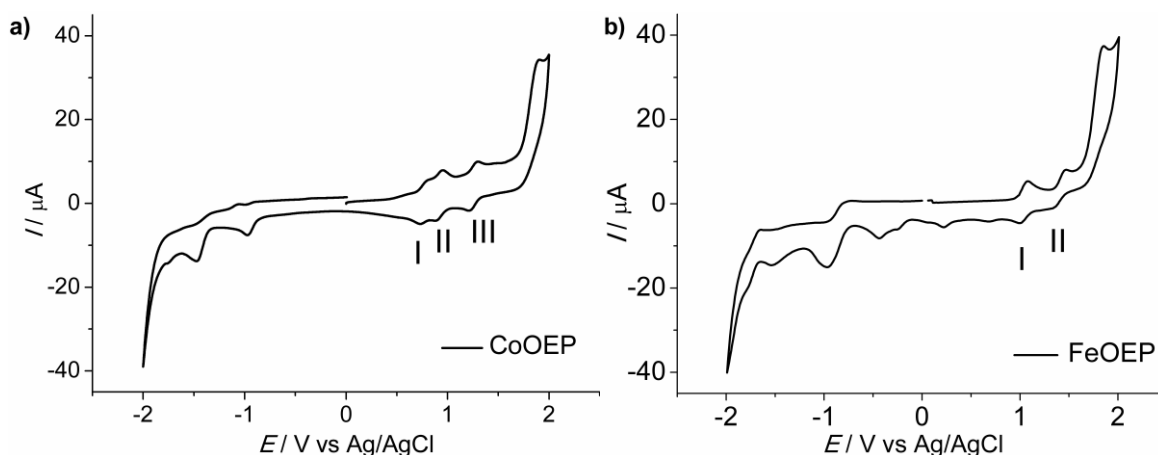


Figure 2. Voltammetric profile of 0.2 mM a) cobalt and b) iron octaethylporphyrins, in 0.1 M tetra-n-butylammonium perchlorate dissolved in dichloromethane. Measurement on glassy carbon electrode, argon atmosphere. $\nu = 100 \text{ mV}\cdot\text{s}^{-1}$.

In Figure 3, the voltammetric profile of the electrodes modified with the porphyrins towards ORR is shown. It can be observed that the GCCo-Fe 1:1 system is the most electroactive towards this reaction, showing a reduction potential displacement (of ca. 200 mV) to positive values. The next ones in terms of activity are GCCo, GCFe and finally the non-modified-GC.

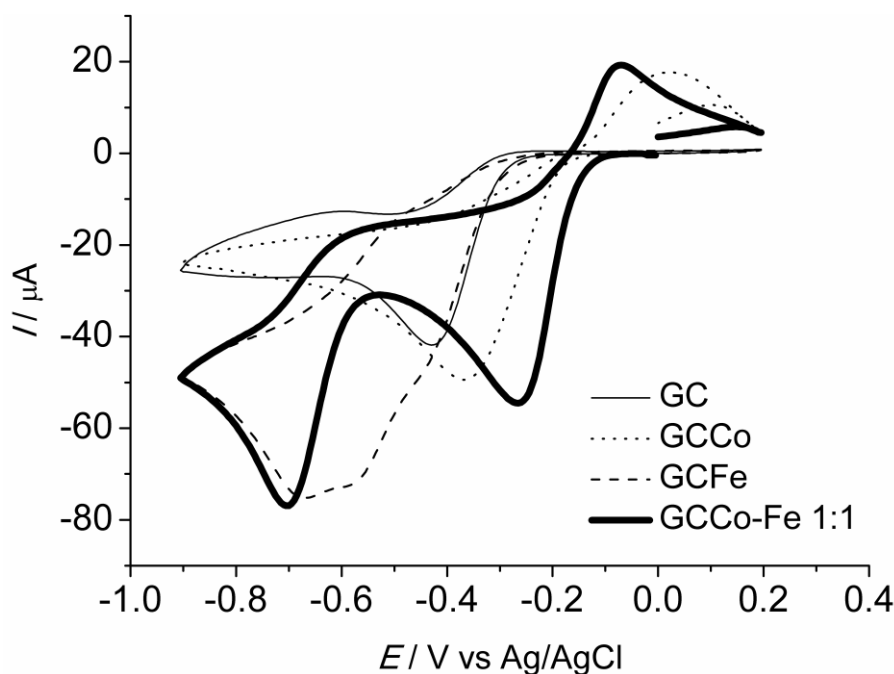


Figure 3. Voltammetric profile for different systems obtained: bare GC (thin continuous line), GCCo (dotted line), GCFe (segmented line), GCCo-Fe 1:1 (thick continuous line) in 0.1 M NaOH saturated with O_2 . $\nu = 100 \text{ mV}\cdot\text{s}^{-1}$.

In Figure 3, it can be seen that the system modified with mixtures of both porphyrins at equal volumetric proportions (GCCo-Fe 1:1) presents two reduction processes of similar charge that would correspond to electron transfer in two active sites of different nature given the presence of different metal centers (Co and Fe). The peak centered at -0.7 V can be attributed to the reduction catalyzed by the redox mediator $\text{Fe}^{\text{III}}/\text{Fe}^{\text{II}}$ while the peak centered at -0.25 V can be attributed to the reduction

catalyzed by the redox mediator $\text{Co}^{\text{III}}/\text{Co}^{\text{II}}$. In this case, there is a shift of the $\text{Co}^{\text{III}}/\text{Co}^{\text{II}}$ toward positive potentials due to the presence of the Fe porphyrin. Although the position of the peaks does not specifically match the one shown in Figure 2, it must be remembered that the medium is different and therefore there is a potential displacement in the involved redox processes. On the other hand, it is not possible to compare the oxygen reduction potentials in aqueous media with the redox couples potentials in dichloromethane because the solubility of porphyrins in water is practically nonexistent and consequently no redox processes attributable to porphyrins in the electrodes modified in aqueous media can be observed. It is interesting to note in Figure 3 the profile corresponding to each complex separately. It can be observed that the GCCo modified system presents an anodic signal at 0 V of less charge than the single cathodic signal that presents a peak potential approximately at -0.35 V. Moreover, GCFe does not present this anodic signal and its cathodic response is a wide signal that begins with the GC response that later reaches a kind of plateau or signal with two maximums at approximately -0.55 V and -0.7 V. When both porphyrins are mixed, the signal is completely different to the sum of the response of each porphyrin in particular showing the synergic effect. The anodic signal that would correspond to the response of GCCo can be observed but at less positive potentials. Two clear and separated cathodic responses appear, the one that would correspond to GCCo is displaced towards positive potentials, the non-modified GC response disappears, and the second cathodic signal appears (which corresponds to the response of GCFe centered at -0.7 V). It is interesting to note two factors in the response of the porphyrin mixture. The first one has to do with the coating. The voltammetric results suggest that the electrode is homogeneously covered with the porphyrin mixture, the cathodic charge in each peak is similar, indicating approximately equimolar amounts of each porphyrin. In the second place, the change of potentials at which the processes occur indicates synergy in the action of the porphyrin mixture as ORR electrocatalysts.

Both catalysts, CoOEP and FeOEP, perform as redox mediators, meaning that by reducing they are able to transfer (simultaneously or not) the electron to the species that they have coordinated, achieving that it receives one electron at the potential where the metal of each porphyrin or the metal-oxygen adduct of each porphyrin is reduced, and therefore shifting the potential towards lower values compared to bare electrode [27].

Moreover, for the oxygen to directly reduce to water, it is necessary that each oxygen atom anchors to an active site at the catalyzer, so that when the negative charge enters to this doubly coordinated oxygen, the O=O bond weakens allowing the breaking of the bond and the formation of water. As shown in Figure 4, by adding hydrogen peroxide instead of oxygen to the solution, again two cathodic signals can be observed in the same potential zones where the oxygen reduction occurs. This clearly indicates that at those potentials the hydrogen peroxide reduces to form water, hence what happens when oxygen is added to the solution is the obtaining of water at each of those cathodic potentials probably by a 2+2 electrons transfer. When the same test with peroxide is carried out on non-modified GC, it is observed that there is no response towards the peroxide reduction, which is coherent with the fact that the GC does not reduce oxygen to water (see Figure S2 of the supplementary material), and therefore in presence of hydrogen peroxide there would not be a response. In this way, in this case the same active sites would be being used for both reductions. This indicates that in the first cathodic process, whose peak is around -0.25 V, the active site can reduce

oxygen and also hydrogen peroxide. The same occurs with the peak situated at -0.7 V. If the oxygen reduction were carried out by a two-electrode mechanism to generate hydrogen peroxide, the same active site would be capable of immediately reduce the peroxide to water. Consequently, regardless it is a process of 2 electrons + 2 electrons, or directly 4 electrons, in each reduction peak the result is water and not hydrogen peroxide.

It is interesting to point out that the system GCCo (Figure 3) generates the appearance of an oxidation peak at the anodic zone that is increased in the hydrogen peroxide reduction by using the system GCCo-Fe 1:1 (Figure 4). This peak could correspond to the porphyrin central metal oxidation, from Co^{II} to Co^{III} [9,28,29]. When the oxygen binds to a Co^{II} center, the reduction is produced and the intermediate $\text{Co}^{\text{III}}(\text{O}_2^{\cdot-})$ is generated. This adduct can bind to another Co center to favor its stabilization [30]. When the hydrogen peroxide reduction happens, the formation of a peroxo bridge between two Co^{III} complexes is favored, what could be observed as an increase in the concentration of the Co^{III} species, as product of its stabilization. The oxidation produces Co^{III} complexes but generally the oxygen action initially derives on peroxo-binuclear species [29,30] due to the instability of the intermediates. This anodic peak would correspond to the formation of Co^{III} peroxo-binuclear species. Those species would be responsible for the oxygen reduction via 4 electrons [9] when reduced. It is known that, generally, cobalt complexes promote the oxygen reduction via 2 electrons, resulting in H_2O_2 as main product [4], but there are studies that demonstrate that the ORR can occur via 4 electrons by the use of Co complexes [9,10,30-33], which agrees with the appearance of the anodic process and our results.

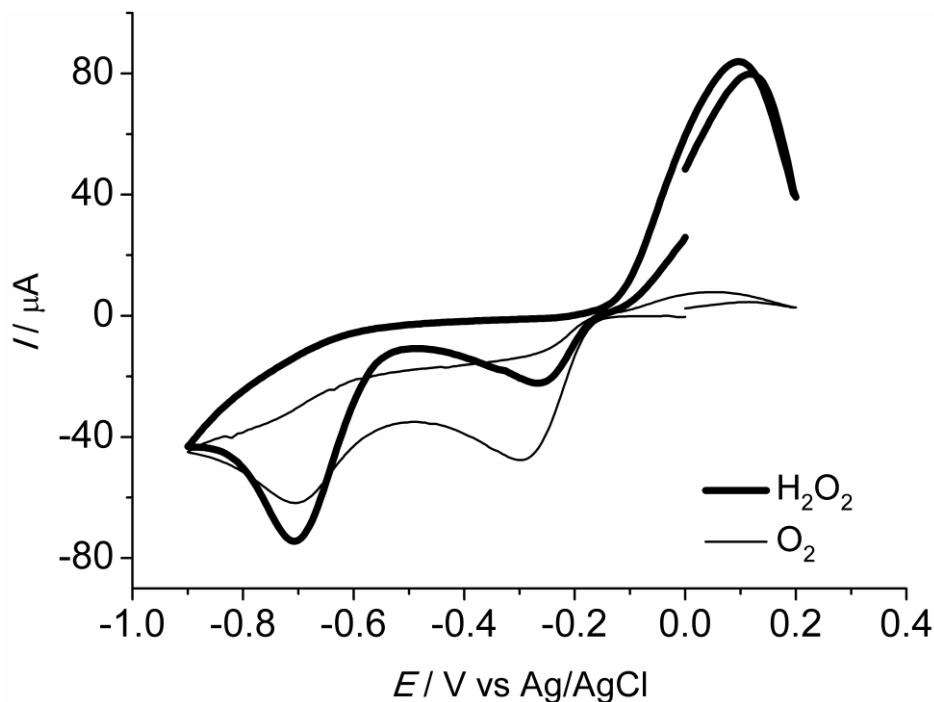


Figure 4. Voltammetric responses for the system GCCo-Fe 1:1 in 0.1 M NaOH solution containing 0.01 M H_2O_2 saturated by Ar (thick line) and in 0.1 M NaOH saturated with O_2 (thin line). $\nu = 100 \text{ mV} \cdot \text{s}^{-1}$.

When the system GCCo-Fe 1:1 is used, the appearance of this anodic process is moved towards more negative potential values (Figure 3). This catalysis is due to the presence of the Fe complex in the mixture that would facilitate the formation of these peroxo-binuclear Co^{III} complexes. A possible explanation for the synergic phenomenon observed could be that the redox reaction between Co^{III} and Fe^{II} is spontaneous, simultaneously producing the reduction of Co^{III} to Co^{II} ($E^\circ = 1.92 \text{ V}$) and the oxidation of Fe^{II} to Fe^{III} ($E^\circ = 0.771 \text{ V}$) [34]. In this way, the interaction between two close sites of Fe^{II} and Co^{III} will generate an electron shift from Fe to Co. So, the higher charge density in Co, product of the interaction with Fe at lower potentials than those expected in the absence of Fe, will allow the oxidation at lower potential.

In this way, the intermediate species $\text{Co}^{\text{III}}(\text{O}_2^{\cdot-})$ will be generated more easily, requiring only a close interaction between both Co and Fe metallic sites. This interaction can be given through the ligands of the porphyrins, since they present a system of aromatic rings [35] that would allow relocating the charge of both centers through π interactions [36-38].

All the above would account for the anodic charge potential displacement towards less positive potentials in presence of the porphyrin mixture and the displacement of the first reduction peak to more positive potentials given the lower energetic requirement to reduce the species thanks to the Fe metallic center. This also explains the movement of the second reduction peak towards more negative values, because of the difficulty to reduce to one species since it is transferring its charge density to Co^{III} .

In Figure 5, the voltammetric responses for systems modified with mixtures of CoOEP and FeOEP are shown, but this time in different volumetric proportions, in which it can be observed a higher activity when GCCo-Fe 1:1 is used, then GCCo-Fe 2:1, and finally GCFE-Co 2:1. The fact that the voltammetric profiles are slightly different verifies the modification with the different mixes and indicates that by varying the composition of both complexes a different arrangement of both porphyrins is obtained on the electrode surface. Also, taking into account the possible negative charge shift from Fe to Co previously mentioned, equivalent amounts of both complexes would be needed so this process can happen in a stoichiometric manner, what would be proven by the activity increase when the proportion 1:1 is used. If the voltammetric responses for the porphyrin mixes are observed (Figure 5), it is possible to notice that in all the cases the appearance of an anodic oxidation peak is generated, just as it happened when the system GCCo (Figure 3) was employed. This explains that, in the case of the mixtures prepared, the oxidation of Co^{II} to Co^{III} would also be taking place, allowing in this way the ORR via 4 electrons. When the system GCCo-Fe 1:1 is used, the anodic zone shows a displacement of potential of the first peak towards more positive values, indicating that is energetically more favorable in comparison to the other mixtures.

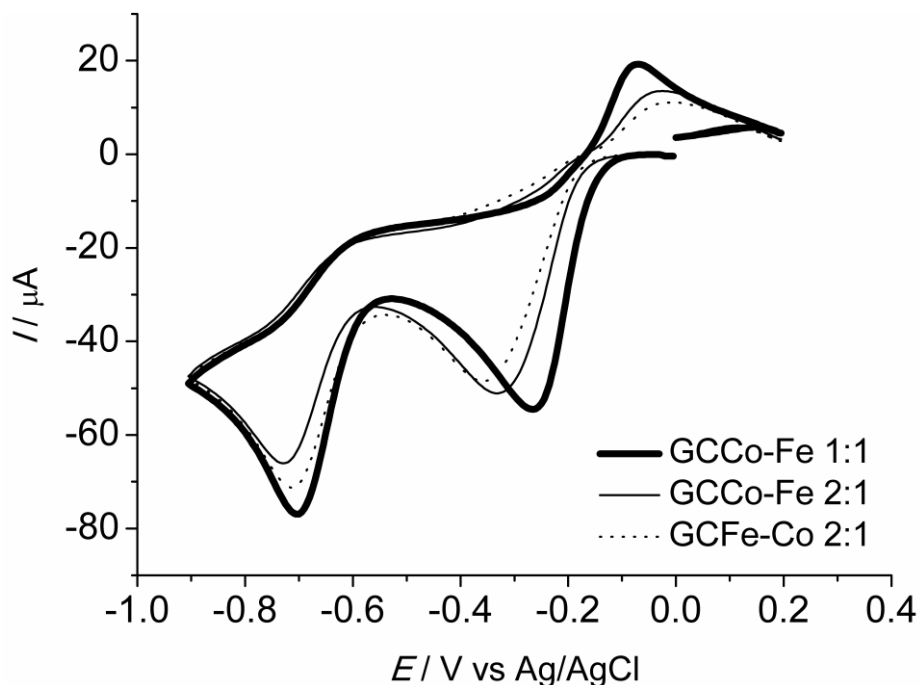


Figure 5. Voltammetric responses for different systems obtained: GCCo-Fe 1:1 (thick line), GCCo-Fe 2:1 (thin line), GCFe-Co 2:1 (dotted line) in 0.1 M NaOH saturated with O_2 . $\nu = 100 \text{ mV}\cdot\text{s}^{-1}$.

3.2. Kinetic studies

The kinetic studies were carried out by using the more active system obtained (GCCo-Fe 1:1) towards the ORR. The control type of the system is obtained from Figure 6a in which it can be observed a linear correlation coefficient (R^2 close to 1) by studying the peak current (I_p) versus the square root of the scan rate ($\nu^{1/2}$). From these data, it is possible to observe that the linear correlations do not pass through zero, indicating some difficulty in the diffusion that is coherent with the porous surface of the covered glassy carbon. In fact, the system is diffusional in its control but considering that the diffusion in the inner electrode is not a semi-infinite linear diffusion. On the other hand, the reaction is completely irreversible allowing using the Randles-Sevcik equation as follows. The number of electrons transferred in the reaction (n) for irreversible and diffusion-controlled systems can be calculated through a mathematical approximation that corresponds to the Randles-Sevcik equation [39], which relates I_p vs $\nu^{1/2}$ and is expressed in the following way:

$$I_p = (2,99 \cdot 10^5) n [(1 - \alpha)n_a]^{1/2} C_o A D_o^{1/2} \nu^{1/2} \quad (1)$$

Here, α is the charge transfer coefficient, n_a is the number of electrons transferred at the rate-determining step in the reaction, D_o is the diffusion coefficient ($2 \cdot 10^{-5} \text{ cm}^2\text{s}^{-1}$) [40], C_o is the oxygen saturation concentration in water ($3.54 \cdot 10^{-4} \text{ mol}\cdot\text{L}^{-1} = 3.54 \cdot 10^{-7} \text{ mol cm}^{-3}$) [41], A is the effective area on the surface of the working electrode and it can be calculated in the following way through the values of image surface area and image projected data, obtained by AFM measurements (see Figure S3 and Table S2 of the supplementary material).

$$\text{effective area} = \left(\frac{\text{Image surface area}}{\text{Image projected area}} \right) \cdot (\text{geometric area})$$

$$\text{effective area} = \left(\frac{101 \mu\text{m}^2}{100 \mu\text{m}^2} \right) \cdot 0.07 \text{ cm}^2 = 0.071 \text{ cm}^2 \quad (2)$$

From the slope in Figure 6a, it can be obtained that for the first reduction process (close to -0.2 V), the value of the slope $I_p/v^{1/2}$ is $145.5 \cdot 10^{-6} \text{ A (Vs}^{-1})$. The value of $[(1 - \alpha)n_a]^{1/2}$ is calculated considering the following equation based on the difference between the peak potential E_p and the half-peak potential $E_{p/2}$ [34,42].

$$(1 - \alpha)n_a = 0.0477 \text{ V} / (E_p - E_{p/2}) \quad (3)$$

In this case, $[(1 - \alpha)n_a]^{1/2} = 0.967$. Applying these values to the Randles-Sevcik equation (1), it is obtained that the number of electrons transferred (n) is 4.4 for the first reduction process (centered at -0.25 V). In an analogous way, the number of electrons transferred for the second reduction process (close to -0.7 V) is calculated considering the slope of the Figure 6b ($135.5 \cdot 10^{-6} \text{ A(Vs}^{-1})$) and the value of $[(1 - \alpha)n_a]^{1/2} = 0.958$. Replacing these values in the Randles-Sevcik equation (1), it is obtained that for the second reduction process the number of electrons transferred (n) is 4.2.

Therefore, using the system GCCo-Fe 1:1, it was obtained by means of calculations that for both reduction processes the number of transferred electrons is 4, a fact that would prove the observed and described in Figure 4.

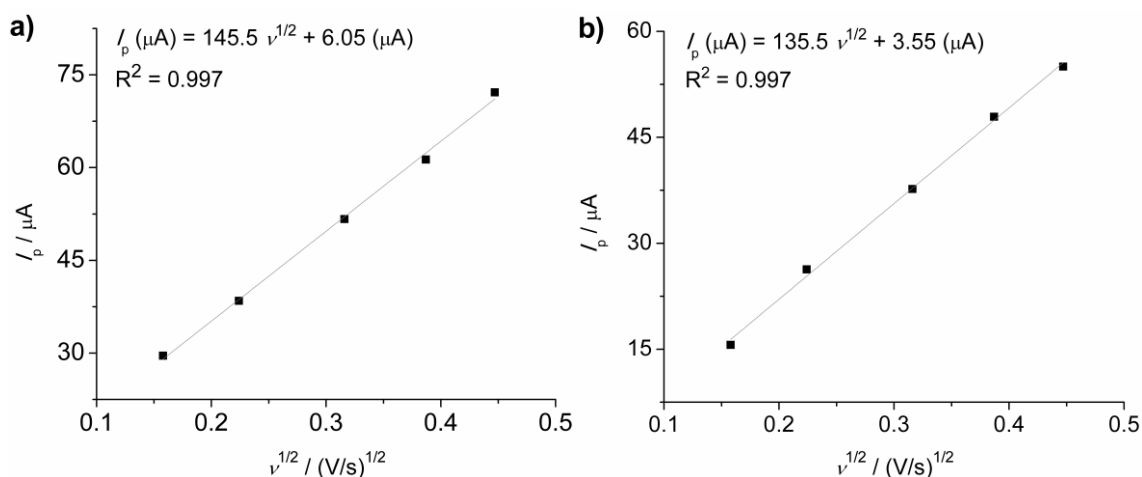


Figure 6. Study of scan rate for a) the first oxygen reduction process, centered at -0.25 V and for b) the second oxygen reduction process, centered at -0.7 V.

In this sense, even if other similar systems previously reported [9,43] present comparable reduction overpotentials, the system here obtained presents two active sites which are capable of reduce oxygen via 4-electrons, due the presence of the mixture of iron and cobalt porphyrins. Also, most of the reported systems are not able to reduce oxygen directly to water but to peroxide via 2-electrons. Considering this, the obtained system possesses the special feature of having two active sites to produce water from molecular oxygen.

3.3. EIS Characterization

The study was carried out by Electrochemical Impedance Spectroscopy (EIS). Impedance is a term that describes the electric resistance [44], allowing for the electric characterization of the different systems generated. Figure 7 shows the Nyquist plot obtained from the systems in study and the respective equivalent circuits (Figure 7 inserted). R_s is the solution resistance, R_{ct} is the charge transfer resistance, C is the capacitance, W is Warburg impedance, and CPE are the constant phase elements. It is important to consider that when the R_{ct} are lower, the charge transference occurs more easily [44]. In the case of the modified systems, it is probable to find two elements of charge transfer resistance. This is due to the existence of an intrinsic resistance corresponding to the GC surface (R_{ct2}), while R_{ct1} corresponds to the resistance of the new material formed in the GC.

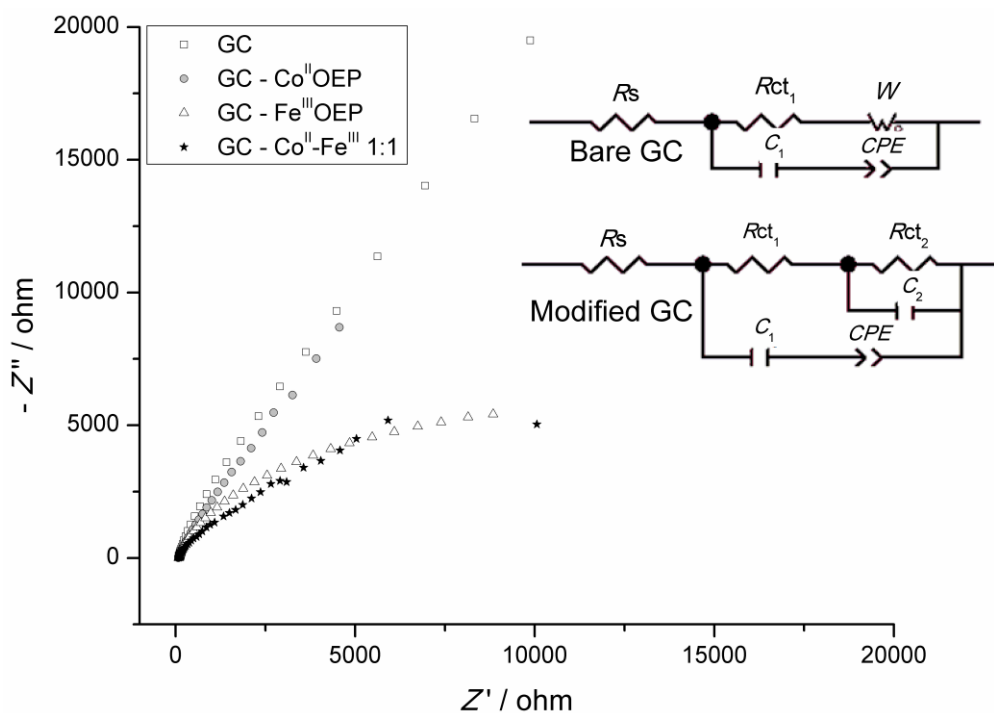


Figure 7. Nyquist plot with the respective equivalent circuits for bare GC and modified GC systems. R_s is the solution resistance, R_{ct} is the charge transfer resistance, C is capacitance, W is Warburg impedance, and CPE are constant phase elements.

It is interesting from data that the system GCCo-Fe 1:1 is more similar in its electric behavior to the system GCFe. However, all the modified systems are explained by the same equivalent circuit that has a difference in the second parallel component that corresponds to a less homogenous surface compared to the GC.

Table 1. Parameters obtained by EIS, corresponding to bare GC and to modified GC systems.

System	R_s / Ω	R_{ct1} / Ω	R_{ct2} / Ω
GC	87.82	39786	-
GCCo	80.31	16178	37745
GCFe	91.54	8227	5868
GCCo-Fe 1:1	85.78	5574	8731

Table 1 shows that bare GC presents the highest R_{ct1} value, followed by GCCo, GCFe, and finally GCCo-Fe 1:1, being this last one the one that presents the lowest resistance to the charge transfer. This indicates that by generating a GCCo-Fe 1:1 modified electrode it is possible to improve the electric properties of this newly formed material. This new material, more conductive is probably due to the stronger interactions among the π interactions of the Fe and Co ligands. This result agrees with the assumption of a strong interaction between Co and Fe centers that contribute to the synergic effects observed in the electrocatalysis.

Based upon the foregoing, the electrochemical impedance spectroscopy (EIS) studies indicate that the porphyrins enhance the conductivity, making the electron transfer faster compared to non-modified GC. Besides, the modified systems present more porosity and are less homogeneous than the non-modified GC, a fact that is clear from the different equivalent circuits for each electrode. These morphological differences can also be seen through AFM studies. It can be observed that bare GC and the modified electrodes (Figure S3 of the supplementary material) are different among themselves and present variations on the R_q values (Table S2 of the supplementary material). The system GCCo-Fe 1:1 is the one that shows the highest R_q value, accounting for a higher surface roughness. This roughness values are coherent with the electrocatalytical data in terms of currents obtained for the different systems, confirming that, in fact, for the system GCCo-Fe 1:1 both porphyrins are deposited in a proportional manner on the GC surface. It is interesting to note that this system, GCCo-Fe 1:1, presents important morphological differences regarding the surfaces modified with CoOEP and FeOEP, indicating that it the generation of a completely different material has been accomplished.

4. CONCLUSIONS

A new material was obtained, compound of GC and a mixture of Co^{II} and Fe^{III} octaethylporphyrins in equal volumetric proportions. This new system (GCCo-Fe 1:1) is more active towards ORR, being energetically more favorable than the GCCo and GCFe systems, separately and in relation to other mixtures analyzed. The system GCCo-Fe 1:1 has the ability to reduce O_2 by two processes of reduction via 4 electrons each one, with the generation of H_2O (probably going through H_2O_2) in two active sites of different nature. Through AFM, it was determined that GCCo-Fe 1:1 presents important morphological differences compared to the other generated systems. Also, by EIS it was obtained that GCCo-Fe 1:1 is the modified system that presents the best electric characteristics, due to its low charge transfer resistance.

ACKNOWLEDGEMENTS

The authors would like to acknowledge the financial support provided by FONDECYT Project No.: 1170340 and No.: 1160324. M.J.A. acknowledges Dicyt-Usach financial support.

SUPPLEMENTARY MATERIAL:

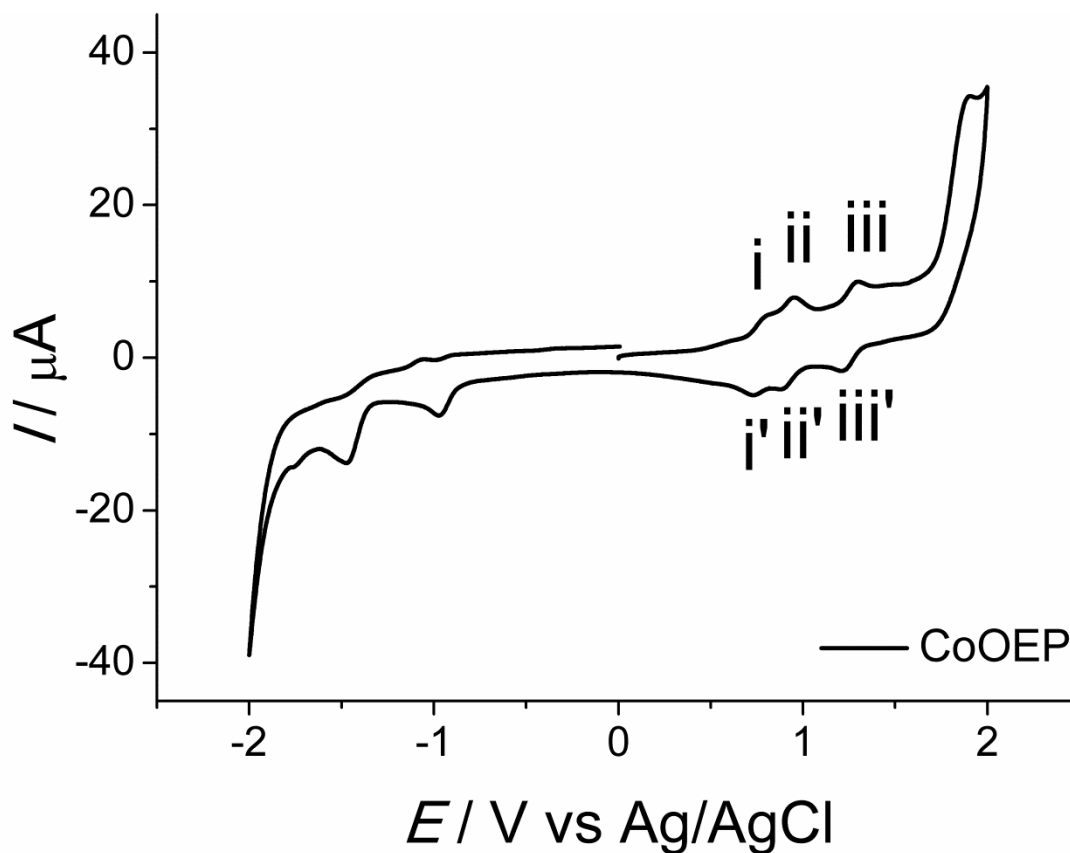


Figure S1. Peak assignment for 0.2 mM cobalt octaethylporphyrin in dichloromethane and tetra-n-butylammonium perchlorate 0,1 M solution as supporting electrolyte. Measurement on glassy carbon saturated with Ar. $v = 100 \text{ mV} \cdot \text{s}^{-1}$.

Table S1. Integrated areas for the peaks in Figure S1.

Peaks	Area / $\text{A} \cdot \text{V}^{-1}$	Peak sum	Area sum / $\text{A} \cdot \text{V}^{-1}$
i + ii	$2,2860 \cdot 10^{-6}$		
i' + ii'	$1,5478 \cdot 10^{-6}$	i + ii + i' + ii'	$3,833 \cdot 10^{-6}$
iii	$3,6415 \cdot 10^{-6}$		
iii'	$2,6041 \cdot 10^{-7}$	iii + iii'	$3,901 \cdot 10^{-6}$

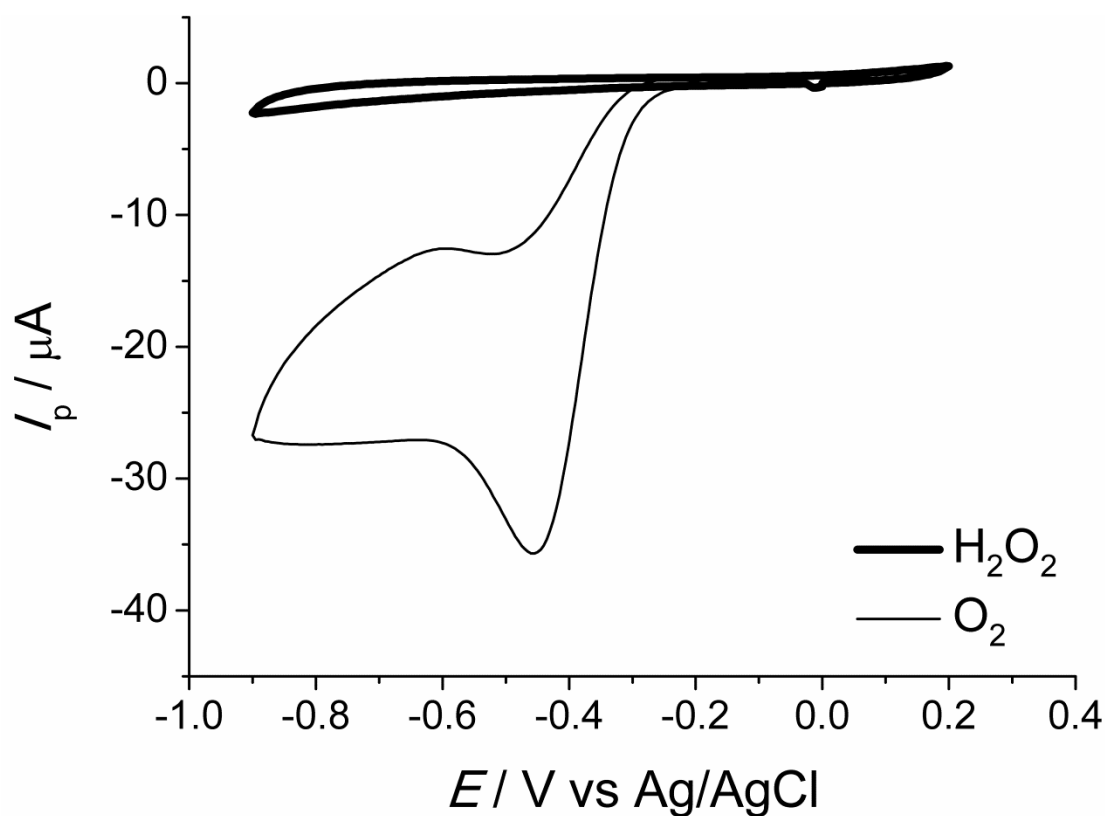


Figure S2. Voltammetric responses for bare GC in solution H_2O_2 0.01 M saturated with Ar (thick line) and in NaOH 0.1 M saturated with O_2 (thin line). $v = 100 \text{ mV}\cdot\text{s}^{-1}$.

Table S2. R_q values, image surface area and image projected area, corresponding to bare GC and modified systems, obtained from Figure S3.

System	R_q value (nm)	Image surface area (μm^2)	Image projected area (μm^2)
GC	4,63	100	100
$\text{GCCo}^{\text{II}}\text{OEP}$	9,35	100	100
$\text{GCFe}^{\text{III}}\text{OEP}$	4,71	100	100
$\text{GCCo}^{\text{II}}\text{-Fe}^{\text{III}}$ 1:1	11.3	101	100

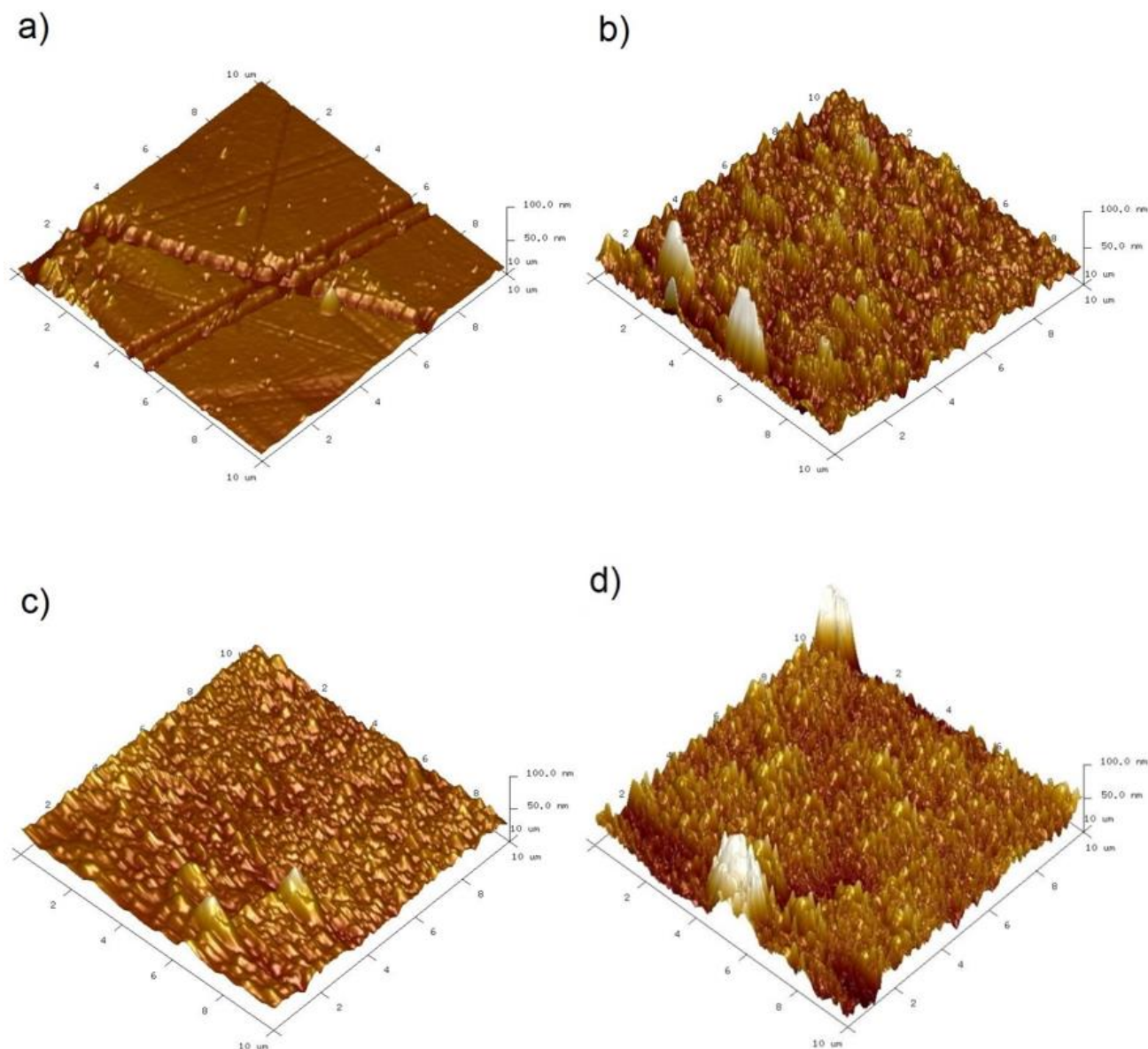


Figure S3. AFM images for a) bare GC, b) GCCo^{II} , c) GCFe^{III} , d) $\text{GCCo}^{\text{II}}\text{-Fe}^{\text{III}}$ 1:1.

References

1. J. Zhang, PEM fuel cell electrocatalysts and catalyst layers: fundamentals and applications. Springer Science & Business Media, (2008) New York, United States.
2. A.R. West, Solid state chemistry and its applications. John Wiley & Sons, (2007) New York, United States.
3. A.A. Gewirth and M.S. Thorum, *Inorg Chem* 49 (2010) 3557.
4. J.H. Zagal and F. Bedioui, Electrochemistry of N_4 Macrocyclic Metal Complexes: Volume 1: Energy. Springer (2016) New York, United States.
5. S. Ferguson-Miller and C.T. Babcock, *Chem Rev* 96 (1966) 2889.
6. G.T. Babcock and M. Wikstrom, *Nature* 356 (1992) 301.

7. M.M. Markovic, T.J. Schmidt, V. Stamenkovic, P.N. Ross, *Fuel Cells* 1 (2001) 105.
8. B. Steele and A. Heinzl, *Nature* 414 (2001) 345.
9. C. Canales and G. Ramírez, *Electrochim Acta* 173 (2015) 636.
10. C. Canales, L. Gidi, G. Ramírez, *Int J Electrochem Sci* 10 (2015) 1684
11. S. Hebié, M. Bayo-Bangoura, K. Bayo, K. Servat, C. Morais, T.W. Napporn and K.B. Kokoh, *J Solid State Electrochem* 20 (2016) 931.
12. C. Shi and F.C. Anson, *Inorg Chem* 29 (1990) 4298.
13. E. Song, C. Shi and F.C. Anson, *Langmuir* 14 (1998) 4315.
14. M.A. Thorseth, C.E. Tornow, E.C.M. Tse and A.A. Gewirth, *Coord Chem Rev* 257 (2003) 130.
15. L.I. Simándi, *Catalytic Activation of Dioxygen by Metal Complexes*, Springer (1992) Netherlands.
16. O. Ikeda, H. Fukuda and H. Tamura, *J Chem Soc Faraday Trans* 1 82 (1986) 1561.
17. A.J. Wallace, B.E. Williamson and D.L. Crittenden, *Can J Chem* 94 (2016) 1163-1168.
18. M. Lucero, M. Riquelme, G. Ramírez, M.C. Goya, A. González-Orive, A. Hernández-Creus, M.C. Arévalo and M.J. Aguirre, *Int J Electrochem Sci* 7 (2012) 234.
19. C. Shi and F.C. Anson, *J Am Chem Soc* 113 (1991) 9564.
20. B. Steiger, C. Shi and F.C. Anson, *Inorg Chem* 32 (1993) 2107.
21. C. Shi and F.C. Anson, *Inorg Chem* 31 (1992) 5078.
22. C. Shi and F.C. Anson, *Inorg Chim Acta* 225 (1994) 215.
23. K.M. Kadish and E. Van Caemelbecke, *J Solid State Electrochem* 7 (2003) 254.
24. K.M. Kadish, K.M. Smith and R. Guilard, *Handbook of porphyrin science. Handbook of porphyrin science*, World Scientific, (2010) Singapore.
25. S. Fukuzumi, *Chem Lett* 37 (2008) 808.
26. M. Khorasani-Motlagh, M. Noroozifar, A. Ghaemi and N. Safari, *J Electroanal Chem* 565 (2004) 115.
27. Z. Shi and J. Zhang, *J Phys Chem C* 111 (2007) 7084.
28. B. Su, I. Hatay, A. Trojanek, Z. Samec, T. Khoury, C.P. Gros, J.M. Barbe, A. Daina, P.A. Carrupt and H.H. Girault, *J Am Chem Soc* 132 (2010) 2655.
29. A. Biloul, F. Coowar, O. Contamin, G. Scarbeck, M. Savy, D. Van Den Ham, J. Riga, J.J. Verbist, *J Electroanal Chem* 350 (1993) 189.
30. J.P. Collman, M. Marrocco, P. Danisevic, C. Koval and F.C. Anson, *J Electroanal Chem* 101 (1979) 117.
31. S. Fukuzumi, S. Mandal, K. Mase, K. Ohkubo, H. Park, J. Benet-Buchholz, W. Nam and A. Llobet, *J Am Chem Soc* 134 (2012) 9906.
32. R. Jasinski, *Nature* 201 (1964) 1212-1213.
33. J.P. Collman, P. Denisevich, Y. Konai, C. Koval, F.C. Anson, *J Am Chem Soc* 102 (1980) 6027.
34. J.A. Bard and L.R. Faulkner, *Electrochemical methods: fundamentals and applications*, Wiley (2000) New York, United States
35. M. Biesaga, K. Pyrzyńska and M. Trojanowicz, *Talanta* 51 (2000) 209
36. Y. Liu, X. Yue, K. Li, J. Qiao, D.P. Wilkinson, J. Zhang, *Coord Chem Rev* 315 (2016) 153.
37. L. Yang, N. Larouche, R. Chenitz, G. Zhang, M. Lefèvre, J.P. Dodelet, *Electrochim Acta* 159 (2015) 184-197.
38. M.L. Rigsby, D.J. Wasylenko, M.L. Pegis, J.M. Mayer, *J Am Chem Soc* 137 (2015) 4296.
39. C. Brett and A.M. Oliveira, *Electrochemistry, Principles, Methods and Applications*, Oxford University Press (1993), UK.
40. M.J. Tham, R.D. Walker Jr, K.E. Gubbins, *J Phys Chem* 74 (1970) 1747.
41. American Public Health Association (APHA), American Water Works Association (AWWA), and Water Environment Federation (WEF), *Standard Methods for the Examination of Water and Wastewater*, United Book Press, Baltimore, Maryland, 2012.
42. C.P. Andrieux and J.M. Saveant, *J Electroanal Chem* 93 (1978) 163.
43. R. Liu, D. Wu, X. Feng and K. Müllen, *Angew Chem* 122 (2010) 2619.

44. X.Z. Yuan, C. Song, H. Wang and J. Zhang, *Electrochemical impedance spectroscopy in PEM fuel cells: fundamentals and applications*, Springer Science & Business Media (2009), New York, United States

© 2018 The Authors. Published by ESG (www.electrochemsci.org). This article is an open access article distributed under the terms and conditions of the Creative Commons Attribution license (<http://creativecommons.org/licenses/by/4.0/>).